Fundamental Limits of Thermal-noise Lossy Bosonic Multiple Access Channel

Evan J.D. Anderson
Optical Sciences
University of Arizona
Tucson Arizona, USA
ejdanderson@optics.arizona.edu

Boulat A. Bash
Electrical & Computer Engineering, Optical Sciences
University of Arizona
Tucson Arizona, USA
boulat@arizona.edu

***Abstract*—Bosonic channels describe quantum-mechanically many practical communication links such as optical, microwave, and radiofrequency. We investigate the maximum rates for the bosonic multiple access channel (MAC) in the presence of thermal noise added by the environment and when the transmitters utilize Gaussian state inputs. We develop an outer bound for the capacity region for the thermal-noise lossy bosonic MAC. We additionally find that the use of coherent states at the transmitters is capacity-achieving in the limits of high and low mean input photon numbers. Furthermore, we verify that coherent states are capacity-achieving for the sum rate of the channel. In the non-asymptotic regime, when a global mean photon-number constraint is imposed on the transmitters, coherent states are the optimal Gaussian state. Surprisingly however, the use of single-mode squeezed states can increase the capacity over that afforded by coherent state encoding when each transmitter is photon number constrained individually.**

I. Introduction

The multiple access channel (MAC) is the principal building block of many practical networks. Indeed, quantum methodologies are being considered for inclusion in 6G wireless networks [1]. Quantum information [2], [3] governs the fundamental limits of physical channels comprising any network, and offers substantial benefits in their performance [4]–[7] and security [8]–[12]. While the MAC has been studied extensively in classical network information theory [13], the quantum perspective has been underexplored. With exception of [14], [15], previous work has largely focused on the quantum channels that act on finite-dimensional qudits [16]–[18]. While recent results focused on coding [19]–[21], entanglement-assisted communication [22]–[25], and secrecy [26], [27], there is a gap in understanding of the fundamental limits of the bosonic multiple access communication with thermal-noise.

While bosonic channels model quantum-mechanically many practical channels (including free-space and fiber optical, microwave, and radiofrequency (RF)), they are particularly useful in optical communications. This is because noises of quantum-mechanical origin limit the performance of advanced high-sensitivity photodetection systems [28]–[30] and the bosonic MAC in particular accurately represents high-speed optical interconnects between and within silicon microchips. Furthermore, quantum methodology includes resources such as squeezed states, shared entanglement, and joint detection receivers that can substantially increase communication capacity. Indeed, the bosonic channel model allows the fundamental limits in throughput and security to be explored by lifting all the assumptions on the transceiver and the adversary except those allowed by the laws of physics. Previous work developed and analyzed the pure-loss bosonic MAC when no excess noise was injected by the environment and the transmitters were restricted to Gaussian inputs [14], [15]. However, such a model does not completely describe practical communication systems as it does not take into account noise in the system. Progress has also been made on the use of entanglement-assistance in the bosonic MAC [22], but the capacity region for the unassisted thermal-noise lossy bosonic MAC still remains underexplored.

We present a model that allows for thermal noise from the environment to be injected into the system. This model allows us to analyze the thermal-noise lossy bosonic MAC via development of maximum rates when Gaussian state inputs are used at the receivers. It additionally allows for the investigation of capacity bounds when asymptotically large and small mean photon number at the transmitters are employed. The inclusion of thermal noise and understanding the limit of low signal power are essential in performing covert communication analysis where an adversary is unable to distinguish between a signal from the transmitter(s) and background noise [10]–[12], [31]–[34]. In evaluating the asymptotic limits of high and low mean photon number at the inputs, we find that coherent states are capacity-achieving (Lemmas 1 and 2, respectively). However, in the finite mean photon-number regime we find that the use of single-mode squeezed states can be beneficial over the use of coherent states unless there is a global mean photon-number constraint at the transmitters in which case coherent states are the optimal Gaussian states (Section III-C).

After formally defining our channel model and stating necessary previous technical results in Section II, in Section III we build on [14], [15] to develop the maximum rates for the lossy thermal-noise bosonic MAC when the transmitters are limited to Gaussian inputs. We conclude in Section IV with discussion of the implications of our results on future work.

This material is based upon work supported by the National Science Foundation under Grant No. CCF-2006679.

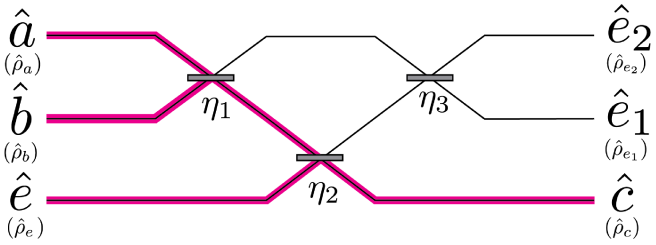

Fig. 1. The generalized three-input, three-output, lossy thermal-noise MAC modeled by beamsplitters with transmissivity η_1, η_2, η_3, an assumed known phase shift set to zero for each beamsplitter, and modal input and output operators $\hat{a}, \hat{b}, \hat{e}, \hat{e}_1, \hat{e}_2, \hat{c}$. Input modal annihilation operators $\hat{a}$ and $\hat{b}$ represent transmitters Alice and Bob while the third $\hat{e}$ is the environment. The receiver, Charlie, is modeled by output modal annihilation operator $\hat{c}$ while $\hat{e}_1, \hat{e}_2$ account for photon loss to the environment. The path photons take from each of the input modes and arrive at the receiver is highlighted.

II. Preliminaries

A. Thermal-Noise Bosonic MAC

The pure-loss channel analyzed by Yen and Shapiro in [14], [15] consists of two input ports, (Alice and Bob), two output ports (Charlie and the environment) and a single beamsplitter. However, the applications of this channel in [14], [15] are limited to systems that are not afflicted by excess thermal noise. Thus, we analyze a richer model via the inclusion of thermal noise. This channel is depicted in Fig. 1. Transmitters are given by modes $\hat{a}, \hat{b}$, and the environment mode, $\hat{e}$, can inject thermal noise. This model requires three beamsplitters η_1, η_2, and η_3 [35], [36] where we ignore phase shifts as is customary in the literature. The output modes consist of the receiver Charlie, $\hat{c}$, and two environment modes, $\hat{e}_1$ and $\hat{e}_2$, which account for photon loss to the environment when traced out. The modal relationship between the input modes and the output mode $\hat{c}$ is given by $\hat{c} = \sqrt{\eta_1\eta_2}\hat{a} + \sqrt{(1-\eta_1)\eta_2}\hat{b} + \sqrt{1-\eta_2}\hat{e}$. This model can be generalized to $K > 2$ transmitters [35], [36]. Here, we focus on $K = 2$ as seen in Fig. 1.

A $((2^{nR_A}, 2^{nR_B}), n)$ code for the two-input MAC includes two input encoders and an output decoder. Alice and Bob independently encode their messages W_A and W_B respectively into length n codewords. Charlie then decodes and estimates the message pair as $(\hat{W}_A, \hat{W}_B)$. The probability of error is then $P_e = P((\hat{W}_A, \hat{W}_B) \neq (W_A, W_B))$. A rate pair (R_A, R_B) is *achievable* if there exists a sequence of $((2^{nR_A}, 2^{nR_B}), n)$ codes such that the $P_e \to 0$ as $n \to \infty$. Winter developed the capacity region for the quantum MAC [16] requiring finite-dimensional Hilbert spaces. Nevertheless, we can use Winter's capacity region by extending it to infinite-dimension Hilbert spaces via a limiting argument [14, Appendix A.1]. The capacity region for the two-sender bosonic MAC is defined as the closure of the union of all achievable rate pairs satisfying

$$R_A \leq \int p_B(\beta) S\left(\bar{\rho}_\beta^B\right) \mathrm{d}\beta - \bar{S} \tag{1}$$

$$R_B \leq \int p_A(\alpha) S\left(\bar{\rho}_\alpha^A\right) \mathrm{d}\alpha - \bar{S} \tag{2}$$

$$R_A + R_B \leq S(\bar{\rho}) - \bar{S} \tag{3}$$

where $\alpha, \beta \in \mathbb{C}$ are Alice and Bob's inputs with distributions $p_A(\alpha), p_B(\beta)$ and $\bar{\rho}_\alpha^A, \bar{\rho}_\beta^B, \bar{\rho}$ (see [37] for their explicit definitions) are the mean density operators at the receiver for Alice, Bob and over the product distribution $p_A(\alpha)p_B(\beta)$ for the joint quantum state $\hat{\rho}(\alpha, \beta)$ at the input ports. Here, $S(\cdot)$ is the von Neumann entropy with $\bar{S} = \int p_A(\alpha)p_B(\beta)S(\hat{\rho}(\alpha,\beta))d\alpha d\beta$.

While the sum-rate capacity, (3), is achieved using coherent-state encoding described in Sec. II-E, only the bounds exist for the individual capacities, the exact solution is an open problem. As such, we consider Gaussian state inputs described next.

B. Gaussian-Input Bosonic MAC

A single-mode quantum state $\hat{\rho}$ is called Gaussian if its Wigner function is of the form [38]:

$$W(\boldsymbol{\mu}) = \frac{\exp\left[-\frac{1}{2}(\boldsymbol{\mu} - \bar{\boldsymbol{\mu}})^\top \boldsymbol{\Sigma}^{-1}(\boldsymbol{\mu} - \bar{\boldsymbol{\mu}})\right]}{2\pi\sqrt{|\boldsymbol{\Sigma}|}}, \tag{4}$$

where $|\mathbf{A}|$ and $\mathbf{A}^\top$ respectively denote the determinant and transpose of matrix $\mathbf{A}$. The mean (displacement) $\bar{\boldsymbol{\mu}} = [\bar{\mu}_1 \ \bar{\mu}_2]^\top$ and covariance matrix $\boldsymbol{\Sigma} = \begin{bmatrix} \sigma_{11}^2 & \sigma_{12}^2 \\ \sigma_{21}^2 & \sigma_{22}^2 \end{bmatrix}$ fully characterize $\hat{\rho}$, and are given for quadrature components $\hat{p} = \mathrm{Im}\,(\hat{a})$ and $\hat{q} = \mathrm{Re}\,(\hat{a})$ of the annihilation operator $\hat{a}$. We do not employ entanglement between quadratures, setting $\sigma_{12}^2 = \sigma_{21}^2 = 0$. States of particular interest to us are:

- vacuum states: $\bar{\boldsymbol{\mu}} = 0, \sigma_{11}^2 = \sigma_{22}^2 = \frac{1}{4}$
- coherent states: $|\bar{\boldsymbol{\mu}}| > 0, \sigma_{11}^2 = \sigma_{22}^2 = \frac{1}{4}$
- single-mode squeezed states: $|\bar{\boldsymbol{\mu}}| \geq 0, \sigma_{11}^2 = \frac{1}{4}e^{2r}, \sigma_{22}^2 = \frac{1}{4}e^{-2r}$ where $r \in \mathbb{R}$ is the squeezing parameter
- thermal states: $\bar{\boldsymbol{\mu}} = 0, \sigma_{11}^2 = \sigma_{22}^2 = \frac{1}{2}(\bar{n}_T + \frac{1}{2})$ where $\bar{n}_T > 0$ is the mean photon number.

The squeezed, coherent, and vacuum states are minimum uncertainty states, the product of their quadrature variances is $\frac{1}{16}$. When squeezing in one quadrature the uncertainty in that quadrature is decreased while the other is increased at the cost of $\frac{1}{4}(e^{2r} + e^{-2r}) - \frac{1}{2} = \frac{1}{2}\cosh(2r) - \frac{1}{2}$ additional photons.

The generalized bosonic channel described in Section II-A preserves Gaussianity. Thus, if Alice and Bob employ Gaussian input states, then Charlie's state is also Gaussian. The covariance matrix at the receiver in terms of the covariance matrices of the three inputs is given by:

$$\boldsymbol{V} = \eta_1\eta_2\boldsymbol{X} + (1-\eta_1)\eta_2\boldsymbol{Y} + (1-\eta_2)\boldsymbol{Z}, \tag{5}$$

where

$$\boldsymbol{X} = \frac{1}{4}\begin{bmatrix} e^{2r_A} & 0 \\ 0 & e^{-2r_A} \end{bmatrix}, \quad \boldsymbol{Y} = \frac{1}{4}\begin{bmatrix} e^{2r_B} & 0 \\ 0 & e^{-2r_B} \end{bmatrix} \tag{6}$$
$$\boldsymbol{Z} = \frac{1}{4}\begin{bmatrix} 2\bar{n}_T + 1 & 0 \\ 0 & 2\bar{n}_T + 1 \end{bmatrix}, \quad \boldsymbol{V} = \begin{bmatrix} V_1 & V_{12} \\ V_{12} & V_2 \end{bmatrix}.$$

Alice and Bob's squeezing parameters are given by r_A, r_B respectively, $\boldsymbol{X}, \boldsymbol{Y}, \boldsymbol{Z}$ are the covariance matrices for the input modes $\hat{a}, \hat{b}$, and $\hat{e}$ respectively, and $\boldsymbol{V}$ is the covariance matrix at Charlie's output mode $\hat{c}$.

Additionally, if Alice is constrained to mean photon number $\bar{n}_A$ and when $r_A \neq 0$, then she can only use $\bar{n}_\alpha = \bar{n}_A - \frac{1}{2}\cosh(2r_A) + \frac{1}{2} = \bar{n}_A - X_1 - X_2 + \frac{1}{2}$ photons for

modulating the mean of her Gaussian input state with the rest of the photons reserved for squeezing. Similarly, for Bob: $\bar{n}_\beta = \bar{n}_B - Y_1 - Y_2 + \frac{1}{2}$. The fractional signal mean photon numbers received by Charlie from Alice and Bob are

$$N_C^A = \eta_1\eta_2\bar{n}_\alpha = \eta_1\eta_2\left(\bar{n}_A - X_1 - X_2 + 1/2\right) \quad (7)$$

$$N_C^B = (1-\eta_1)\eta_2\left(\bar{n}_B - Y_1 - Y_2 + 1/2\right). \quad (8)$$

C. Coherent Receivers

It is useful to examine coherent receivers (homodyne and heterodyne) when considering channel capacity as they are commonly used in practice [38, Section II.E]. Homodyne receivers are maximized with Gaussian inputs, and the sum-rate capacity (3) of squeezed state homodyne detection for the Alice-to-Charlie channel in Fig. 1 is [39, eq. 7.51]

$$C_{\text{hom}} = \frac{1}{2}\log\left(1 + \frac{4(\bar{n}_\alpha + \frac{(1-\eta_1)}{\eta_1}\bar{n}_\beta)}{e^{2r_A} + \frac{(1-\eta_1)}{\eta_1}e^{2r_B} + \frac{1-\eta_2}{\eta_1\eta_2}(1+2\bar{n}_T)}\right). \quad (9)$$

Similarly, coherent states maximize the sum-rate for heterodyne detection, yielding a capacity of [39, eq. 7.43]

$$C_{\text{het}} = \log\left(1 + \frac{\eta_1\bar{n}_A + (1-\eta_1)\bar{n}_B}{1 + \frac{1-\eta_2}{\eta_2}(1+2\bar{n}_T)}\right). \quad (10)$$

Additionally, the individual-user capacities of homodyne and heterodyne detection are given by

$$C_{\text{hetA}} = C_{\text{het}}|_{\bar{n}_B=0}\,, \quad C_{\text{hetB}} = C_{\text{het}}|_{\bar{n}_A=0} \quad (11)$$

$$C_{\text{homA}} = C_{\text{hom}}|_{\bar{n}_B=0}\,, \quad C_{\text{homB}} = C_{\text{hom}}|_{\bar{n}_A=0}\,. \quad (12)$$

D. Quantum Gaussian MAC

Yen and Shapiro extended the Holevo-Sohma-Hirota classical capacity of quantum point-to-point Gaussian channels for squeezed states [4] to two users [14], [15]. The maximum rates of the channel are given by a piecewise function, which we restate here using the following three functions:

$$G_{11}(N, \boldsymbol{V}) = g\left(V_1 + V_2 + N - \frac{1}{2}\right), \quad (13)$$

$$G_{12}(N, \boldsymbol{V})) = g\left(2\left[-\left(\sqrt{\left(\frac{V_1 - V_2}{2}\right)^2 + V_{12}^2} - \frac{N}{2}\right)^2 + \left(\frac{V_1 + V_2 + N}{2}\right)^2\right]^{\frac{1}{2}} - \frac{1}{2}\right), \quad (14)$$

$$G_2(\boldsymbol{V}) = g\left(2|\boldsymbol{V}|^{1/2} - \frac{1}{2}\right) \quad (15)$$

where $g(\cdot)$ is defined as

$$g(x) \equiv (1+x)\log(1+x) - x\log x. \quad (16)$$

The sum rate for the MAC is

$$R_{\text{maxAB}} = \begin{cases} R_{\text{maxAB1}} & \text{if } N_C^{A+B} \geq \sqrt{(V_1 - V_2)^2 + 4V_{12}^2} \\ R_{\text{maxAB2}} & \text{if } N_C^{A+B} < \sqrt{(V_1 - V_2)^2 + 4V_{12}^2} \end{cases} \quad (17)$$

where $N_C^{A+B} = N_C^A + N_C^B$, $R_{\text{maxAB1}} = G_{11}(N_C^{A+B}, \boldsymbol{V}) - G_2(\boldsymbol{V})$, and $R_{\text{maxAB2}} = G_{12}(N_C^{A+B}, \boldsymbol{V}) - G_2(\boldsymbol{V})$. The individual rate is

$$R_{\text{maxA}} = \begin{cases} R_{\text{maxA1}} & \text{if } N_C^{A} \geq \sqrt{(V_1 - V_2)^2 + 4V_{12}^2} \\ R_{\text{maxA2}} & \text{if } N_C^{A} < \sqrt{(V_1 - V_2)^2 + 4V_{12}^2} \end{cases} \quad (18)$$

where $R_{\text{maxA1}} = G_{11}(N_C^A, \boldsymbol{V}) - G_2(\boldsymbol{V})$, and $R_{\text{maxA2}} = G_{12}(N_C^A, \boldsymbol{V}) - G_2(\boldsymbol{V})$. An expression for R_{maxB} is obtained by swapping N_C^A with N_C^B. For the states we are interested in, $V_{12} = 0$ and the threshold in (18) evaluates to $N_C^A \lessgtr |V_1 - V_2|$. A similar condition also holds for (17).

E. Coherent-State Gaussian Random Code

Consider input with block size of M bits and codewords of length n. Then a channel code's rate is $R = M/n$ bits/symbol. Let $\hat{\rho}(\alpha)$ be a coherent state with mean $\alpha \in \mathbb{C}$. Then suppose the encoder generates 2^{nR} codewords for codebook $\mathcal{C} = \{\otimes_{m=1}^n \hat{\rho}_k(\alpha_m)\}_{k=1}^{2^{nR}}$ each according to $p(\otimes_{m=1}^n \hat{\rho}_k(\alpha_m)) = \Pi_{m=1}^n p(\alpha_m)$, where $p(\alpha) = e^{-|\alpha|^2/\bar{n}}/(\pi\bar{n})$ is the circularly-symmetric complex Gaussian distribution, $\otimes_{i=1}^n$ denotes the n-mode tensor product, and $\bar{n}$ is the mean photon number per symbol. Yen and Shapiro showed that such a random code combined with a joint measurement receiver maximizes the sum rate R_{maxAB} for the pure-loss bosonic MAC. Moreover, such encoding also was shown to be optimal for the sum rate for the generalized phase-insensitive bosonic MAC [22]. We employ this code for both transmitters in the next section.

III. Thermal-Noise Lossy Bosonic Multiple Access Channel Capacity

In this section we investigate the capacity for the thermal-noise lossy bosonic MAC and its asymptotic limits.

A. Individual Rate Outer Bounds

It was conjectured in [6] and later proven in [7] that for the point-to-point thermal-noise lossy bosonic channel, the capacity is reached with coherent-state encoding. For a general point-to-point lossy thermal-noise channel, given $\bar{x}$ as the mean photon number of the signal from the transmitter at the receiver and $\bar{y}$ as the mean photon number of the thermal noise at the receiver, the capacity is:

$$C(\bar{x}, \bar{y}) = g(\bar{x} + \bar{y}) - g(\bar{y}). \quad (19)$$

Thus, the capacity of Alice-to-Charlie (point-to-point) channel when Bob inputs vacuum is:

$$C_{\text{A}} = C(\eta_1\eta_2\bar{n}_A, (1-\eta_2)\bar{n}_T). \quad (20)$$

For our two-user thermal-noise MAC, the ultimate upper bound (ub), regardless of input state (Gaussian or otherwise)

for the individual rates ignores the interference from the other user. This corresponds to a nonphysical receiver that can undo the beamsplitter between the two transmitters yielding

$$R_{\mathrm{maxA}} \leq R_{\mathrm{ubA}} = C(\eta_2 \bar{n}_A, (1-\eta_2)\bar{n}_T) \tag{21}$$

$$R_{\mathrm{maxB}} \leq R_{\mathrm{ubB}} = C(\eta_2 \bar{n}_B, (1-\eta_2)\bar{n}_T). \tag{22}$$

B. Asymptotics of Photon-Number Constraints

The sum-rate capacity is achieved through the use of coherent Gaussian states [7], [22],

$$R_A + R_B \leq C(\eta_2(\eta_1 \bar{n}_A + (1-\eta_1)\bar{n}_B), (1-\eta_2)\bar{n}_T), \tag{23}$$

where the RHS is equivalent to substituting coherent states in (17) and $C(\bar{x}, \bar{y})$ is defined in (19). Now, we evaluate the scaling of the individual rate for Alice with respect to the upper bounds in (21) in the case of asymptotically large input power noting that the same process applies for Bob and (22).

Lemma 1: A random code with coherent-state encoding with heterodyne detection achieves the individual rate capacity of the thermal-noise lossy bosonic MAC in the asymptotic limit of large transmitter input power with constant thermal noise.

Proof: For coherent-state inputs ($r_A = r_B = 0$) at Alice and Bob and a heterodyne detector at the receiver, Charlie, the capacities C_{hetA} and C_{hetB} are given by (11). Then

$$\lim_{\bar{n}_A \to \infty} \frac{C_{\mathrm{hetA}}}{R_{\mathrm{ubA}}} = \lim_{\bar{n}_B \to \infty} \frac{C_{\mathrm{hetB}}}{R_{\mathrm{ubB}}} = 1. \tag{24}$$

Evaluation of the limits are performed using L'Hôpital's rule and derived in [37, Appendix A]. Hence, coherent-state encoding with heterodyne detection yields the individual rate upper bounds as $\bar{n}_A \to \infty$ and $\bar{n}_B \to \infty$. ∎

For homodyne detection utilizing coherent states or squeezed states, the scaling of the individual rate for Alice with respect to the upper bound in (21) is evaluated as follows:

$$\lim_{\bar{n}_A \to \infty} \max_{r_A} \lim_{\bar{n}_B \to \infty} \max_{r_B} \frac{C_{\mathrm{hom}}}{R_{\mathrm{ubA}}} = \frac{1}{2}, \tag{25}$$

where the maximization over r_B in the inner limit as $\bar{n}_B \to \infty$ puts all the energy available to Bob into squeezing, that is, optimal $r_B \to -\infty$. This contrasts the pure-loss channel result in [14], [15] where (25) evaluates to unity.

Lemma 2: In the limit of small photon number and constant thermal noise, utilizing a random code with coherent-state encoding at Alice and Bob and a joint detection receiver at Charlie achieves the capacity of the thermal-noise lossy bosonic MAC.

Proof: We evaluate the three cases corresponding to the order in which photon numbers input by Alice and Bob decay to zero.

Case 1. Bob's input photon number decays to zero first:

$$\lim_{\bar{n}_A \to 0} \lim_{\bar{n}_B \to 0} \frac{R_{\mathrm{maxA}}}{C_{\mathrm{A}}} = 1 \tag{26}$$

When Bob's photon number decays to zero first, he effectively has no photons for squeezing guaranteeing that $N_C^A \geq |V_1 - V_2|$ and $R_{\mathrm{maxA}} = R_{\mathrm{maxA1}}$. Hence, the MAC reduces to a point-to-point channel in which Alice's signal photon number is attenuated by an $\eta_1\eta_2$ term and coherent-state encoding achieves the capacity C_{A} in (20). This demonstrates that (21) can be made tighter in the asymptotic limit of small input power. Limits in (26) are evaluated by inspection.

Case 2. Alice's input photon number decays to zero first:

$$\lim_{\bar{n}_B \to 0} \lim_{\bar{n}_A \to 0} \frac{R_{\mathrm{maxA}}}{C_{\mathrm{A}}} = 1 \tag{27}$$

We allow Bob to perform an arbitrary amount of squeezing, setting his squeezing parameter to $r_B = \sinh^{-1}(\sqrt{\bar{n}_B})$. If Alice's input photon number decays to zero first, $N_C^A < |V_1 - V_2|$ and $R_{\mathrm{maxA}} = R_{\mathrm{maxA2}}$. The first limit ($\bar{n}_A \to 0$) is evaluated using a single application of L'Hôpital's rule, yielding a simple expression that allows the second limit ($\bar{n}_B \to 0$) to be evaluated by inspection. Details are in [37, Appendix B1].

Case 3. Alice and Bob's input photon numbers decay to zero simultaneously. Let $\bar{n}_A = a\bar{n}, \bar{n}_B = b\bar{n}$ with arbitrary constants $a, b > 0$. We show that

$$\lim_{\bar{n} \to 0} \frac{R_{\mathrm{maxA}}}{C_{\mathrm{A}}} = 1. \tag{28}$$

First consider $N_C^A \geq |V_1 - V_2|$ when $R_{\mathrm{maxA}} = R_{\mathrm{maxA1}}$. Then any squeezing at Alice is sub-optimal because

$$G_{11}(N_C^A, \boldsymbol{V}) = g\left(\eta_1\eta_2 a\bar{n} + (1-\eta_1)\,\eta_2 b\bar{n} + (1-\eta_2)\bar{n}_T\right)$$

is a function of the total photon number $a\bar{n}$ at Alice and does not depend on squeezing parameter r_A. Furthermore $|\boldsymbol{V}|$ in (15) is minimized for coherent-state input at Alice. Therefore, since $g(\cdot)$ is monotonic, R_{maxA1} is maximized by setting $r_A = 0$. When Bob and Alice both use coherent-state encoding:

$$\lim_{\bar{n} \to 0} \frac{R_{\mathrm{maxA1}}|_{r_A = r_B = 0}}{C_{\mathrm{A}}} = 1. \tag{29}$$

To show that any squeezing at Bob's transmitter cannot help, we first note that the only impact from Bob's transmissions on R_{maxA1} is through transmission of squeezed states. Suppose that Bob is allowed to squeeze arbitrarily. As b is arbitrary, let Bob's squeezing parameter be $r_B = \sinh^{-1}(\sqrt{b\bar{n}})$, and Alice is transmitting an optimal coherent state ($r_A = 0$) as discussed previously. However, the constraint $N_C^A \geq |V_1 - V_2|$ upper bounds b as

$$b_{\mathrm{maxA1}} \leq \frac{\eta_1 - 1 + \sqrt{1 + \eta_1(2 - \eta_1(1 - 4a^2\bar{n}^2))}}{2(1-\eta_1)\bar{n}}. \tag{30}$$

Note that b is dependent on $\bar{n}$. Then, to upper bound Bob's possible arbitrary squeezing, let $b = \kappa b_{\mathrm{maxA1}}$ where κ is arbitray and $\kappa \in [0, 1]$. Hence the limit involving R_{maxA1} becomes

$$\lim_{\bar{n} \to 0} \frac{R_{\mathrm{maxA1}}|_{r_A = 0, r_B = \sinh^{-1}(\sqrt{\kappa b_{\mathrm{maxA1}}\bar{n}})}}{C_{\mathrm{A}}} = 1. \tag{31}$$

Evaluation of the limit involves an application of L'Hôpital's rule and is shown in [37, Appendix B2]. Thus, squeezing does not help when $N_C^A \geq |V_1 - V_2|$.

Now consider $N_C^A < |V_1 - V_2|$ when $R_{\mathrm{maxA}} = R_{\mathrm{maxA2}}$. For Gaussian state inputs, $G_{12}(N_C^A, \boldsymbol{V}) = g(2\sqrt{V_1(\eta_1\eta_2 p_A a\bar{n} + V_2)} - \frac{1}{2})$ for $V_1 > V_2$ (with V_1

and V_2 swapped when $V_2 > V_1$), where $p_A \in [0,1]$ is the fraction of photons Alice uses for displacement and $(1-p_A)$ used for squeezing. Additionally, for coherent-state encoding, $G_{11}(N_C^A, \boldsymbol{V}) = g(\eta_1\eta_2 a\bar{n} + (1-\eta_2)\bar{n}_T)$. Now

$$\lim_{\bar{n}\to 0} \frac{G_{12}(N_C^A, \boldsymbol{V})}{G_{11}(N_C^A, \boldsymbol{V})|_{r_A=r_B=0}} = 1, \tag{32}$$

which is derived using meticulous expansion of the terms and taking their corresponding limit in [37, Appendix B3]. As R_{maxA1} and R_{maxA2} both include $G_2(\boldsymbol{V})$ terms

$$\lim_{\bar{n}\to 0} \frac{R_{\text{maxA2}}}{R_{\text{maxA1}}|_{r_A=r_B=0}} \leq 1. \tag{33}$$

Squeezing by Alice or Bob increases $G_2(\boldsymbol{V})$ as $g(\cdot)$ is monotonic, and when $\bar{n}_T > 0$, $|\boldsymbol{V}|$ is an increasing function of r_A and r_B. Thus, including $G_2(\boldsymbol{V})$ terms causes the numerator of (32) to decay faster than the denominator. Therefore, any squeezing by Alice and Bob in R_{maxA2} is at best equivalent to the optimal rate defined by R_{maxA1} with $r_A = r_B = 0$ in the asymptotic limit of small input power.

Employing Bob's maximum rate R_{maxB} and corresponding $C_{\text{A}} = C((1-\eta_1)\eta_2\bar{n}_B, (1-\eta_2)\bar{n}_T)$ instead of R_{maxA} results in limits above also evaluating to 1 as expected. ■

We note that when we replace R_{maxA} in (28) with coherent or squeezed homodyne or coherent heterodyne capacities, the limit evaluates to zero. Therefore achieving bosonic MAC capacity requires more complex receiver designs.

C. Fixed Mean Photon-Number Constraints

While utilization of coherent states are optimal at both asymptotically high and low input mean photon number, most practical systems operate in a finite mean photon number regime of fixed input power. There are two possible ways to fix the input power, via a global mean photon-number constraint that is spread across all transmitters, and a mean photon-number constraint for each of the individual transmitters.

We first examine the global mean photon number constraint $\bar{n}_S$, for both the transmitters. Let the fractional photon-number constraint for Alice be $\bar{n}_A = s\bar{n}_S$ and likewise for Bob, $\bar{n}_B = (1-s)\bar{n}_S$ where $s \in [0,1]$. As this constraint is global, we assume Alice and Bob can control s. Only the photons Bob uses for squeezing affect Alice's rate as they introduce additional noise in the channel. In this case, we can treat the channel as a point-to-point channel from Alice to Charlie with a mean photon-number constraint $\bar{n}_S$ such that $s\bar{n}_S$ photons are used for the signal and $(1-s)\bar{n}_S$ photons are used for squeezing by the transmitter. As mentioned in Sec. III-A, coherent states are optimal in the point-to-point channel, which corresponds to Alice using all $\bar{n}_S$ photons for displacement, $s = 1$. For the sum rate R_{maxAB}, substituting (5), (7), and (8) into $G_{11}(N, \boldsymbol{V})$ yields $G_{11}(N_C^{A+B}, \boldsymbol{V}) = g(\bar{n}_T + (\bar{n}_B - \bar{n}_T + (\bar{n}_A - \bar{n}_B)\eta_1)\eta_2)$, without squeezing parameter dependence. Similarly, $G_{12}(N_C^{A+B}, \boldsymbol{V})$ is strictly smaller than $G_{11}(N_C^{A+B}, \boldsymbol{V})$. Thus maximization of R_{maxAB} reduces to the minimization of of $G_2(\boldsymbol{V})$, or $|\boldsymbol{V}|$, as $g(\cdot)$ is monotonic. The minimum occurs for coherent-state inputs ($r_A = r_B = 0$) and matches the results in [14], [15], [22].

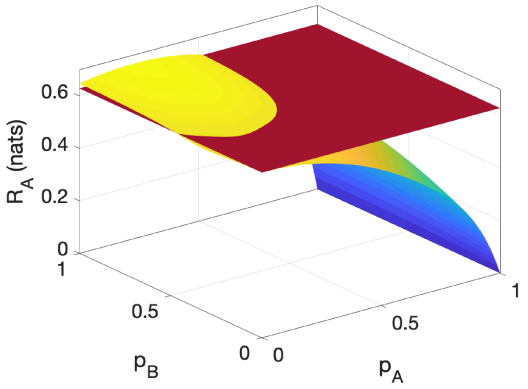

Fig. 2. Individual rates generated for all possible squeezed states given input parameters $\bar{n}_A = 4, \bar{n}_B = 8, \bar{n}_T = 4, \eta_1 = 0.2, \eta_2 = 0.9$. $p_A = \sinh^2(r_A)/\bar{n}_A$ and $p_B = \sinh^2(r_B)/\bar{n}_B$ are fractions of the total photon number utilized for squeezing by Alice and Bob respectively. The dark red plane indicates the rate achieved utilizing coherent-state encoding ($p_A = p_B = 0$) at both transmitters.

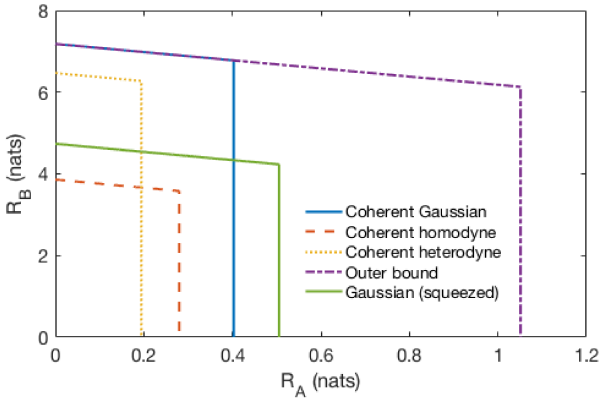

Fig. 3. Capacity region given for rates (17), (18) (and corresponding R_{maxB}) for the use of coherent Gaussian states and joint detection, coherent homodyne, coherent heterodyne detection, Gaussian squeezed states, and the outer bound defined in (21). Here, $\bar{n}_A = 1, \bar{n}_B = 1000, \bar{n}_T = 1, \eta_1 = 0.25, \eta_2 = 0.9$, and in the case of the squeezed state region, $r_A = 0, r_B = 3$.

On the other hand, if the transmitters are under individual mean photon-number constraints i.e. not allowed to share their power, coherent-state encoding does not necessarily maximize the individual rates. While squeezing does not encode information directly, an example of squeezed states outperforming coherent-state encoding is shown in Fig. 2. The non-linear optimization of squeezing parameters is analytically intractable. However, with known channel parameters, a numeric search quickly shows whether squeezing helps and the corresponding values for the squeezing parameters. In Fig. 3 we plot the capacity rate region for coherent homodyne and heterodyne, coherent encoding and squeezed state encoding with optimal joint detection, and the individual rate outer bound in (21). In this example, utilizing squeezed states extends R_A beyond the coherent encoding envelope at the expense of reduced R_B.

IV. Discussion and Conclusion

Given a total mean photon-number constraint on the system, Alice and Bob can do no better than the capacity of coherent-state encoding, allocating all of the power to Alice or Bob depending on the transmission goal. For individual mean photon-number constraints, or when Alice and Bob lack control over total power allocation, Figs. 2 and 3 show that squeezing can improve the individual rates, although an intuitive explanation for this remains elusive. Characterizing the benefit of such "local" quantum enhancement at the transmitters is a compelling direction for future work. It is possible non-Gaussian states can reach the outer bound and further exploration of these states remains an open problem.

In Lemmas 1-2 we prove that in asymptotic regimes of both high and low SNR, coherent-state encoding is optimal. The fact that coherent states are capacity-achieving for asymptotically low mean photon number lays the foundation for performing covert communication analysis and is a logical next step. However, unlike the high SNR regime, neither homodyne nor heterodyne detection are capacity-achieving and other physically realizable receivers should be explored.

Acknowledgment

The authors thank Saikat Guha for insightful discussion.

References

[1] F. Granelli, R. Bassoli, J. Nötzel, F. H. P. Fitzek, H. Boche, and N. L. S. da Fonseca, "A novel architecture for future classical-quantum communication networks," *Wireless Communications and Mobile Computing*, vol. 2022, p. 3770994, Apr 2022.

[2] M. A. Nielsen and I. L. Chuang, *Quantum Computation and Quantum Information*. New York, NY, USA: Cambridge University Press, 2000.

[3] M. Wilde, *Quantum Information Theory*, 2nd ed. Cambridge University Press, 2016.

[4] A. S. Holevo, M. Sohma, and O. Hirota, "Capacity of quantum Gaussian channels," *Phys. Rev. A*, vol. 59, no. 3, pp. 1820–1828, Mar. 1999.

[5] V. Giovannetti, S. Lloyd, L. Maccone, and P. W. Shor, "Broadband channel capacities," *Phys. Rev. A*, vol. 68, p. 062323, Dec. 2003.

[6] V. Giovannetti, S. Guha, S. Lloyd, L. Maccone, and J. H. Shapiro, "Minimum output entropy of bosonic channels: a conjecture," *Phys. Rev. A*, vol. 70, no. 3, p. 032315, Sep. 2004.

[7] V. Giovannetti, R. Garcia-Patron, N. J. Cerf, and A. S. Holevo, "Ultimate communication capacity of quantum optical channels by solving the Gaussian minimum-entropy conjecture," *Nature Photon*, vol. 8, no. 10, pp. 796–800, Oct. 2014.

[8] V. Scarani, H. Bechmann-Pasquinucci, N. J. Cerf, M. Dušek, N. Lütkenhaus, and M. Peev, "The security of practical quantum key distribution," *Rev. Mod. Phys.*, vol. 81, pp. 1301–1350, Sep. 2009.

[9] S. Pirandola, U. L. Andersen, L. Banchi, M. Berta, D. Bunandar, R. Colbeck, D. Englund, T. Gehring, C. Lupo, C. Ottaviani, J. L. Pereira, M. Razavi, J. S. Shaari, M. Tomamichel, V. C. Usenko, G. Vallone, P. Villoresi, and P. Wallden, "Advances in quantum cryptography," *Adv. Opt. Photon.*, vol. 12, no. 4, pp. 1012–1236, Dec 2020.

[10] B. A. Bash, A. H. Gheorghe, M. Patel, J. L. Habif, D. Goeckel, D. Towsley, and S. Guha, "Quantum-secure covert communication on bosonic channels," *Nat. Commun.*, vol. 6, Oct. 2015.

[11] M. S. Bullock, C. N. Gagatsos, S. Guha, and B. A. Bash, "Fundamental limits of quantum-secure covert communication over bosonic channels," *IEEE J. Sel. Areas Commun.*, vol. 38, no. 3, pp. 471–482, Mar. 2020.

[12] C. N. Gagatsos, M. S. Bullock, and B. A. Bash, "Covert capacity of bosonic channels," *IEEE J. Sel. Areas Inf. Theory*, vol. 1, pp. 555–567, 2020.

[13] A. E. Gamal and Y.-H. Kim, *Network Information Theory*. New York, NY, USA: Cambridge University Press, 2012.

[14] B. J. Yen and J. H. Shapiro, "Multiple-access bosonic communications," *Phys. Rev. A*, vol. 72, no. 6, p. 062312, Dec. 2005.

[15] B. J. Yen, "Multiple-user quantum optical communication," Ph.D. dissertation, Massachusetts Institute of Technology, 2005.

[16] A. Winter, "The capacity of the quantum multiple-access channel," *IEEE Trans. Inf. Theory*, vol. 47, no. 7, pp. 3059–3065, 2001.

[17] J. Yard, I. Devetak, and P. Hayden, "Capacity theorems for quantum multiple access channels," in *Proc. IEEE Int. Symp. Inf. Theory (ISIT)*, 2005, pp. 884–888.

[18] R. Ahlswede and N. Cai, *A Strong Converse Theorem for Quantum Multiple Access Channels*. Berlin, Heidelberg: Springer-Verlag, 2006, pp. 460–485.

[19] H. Qi, Q. Wang, and M. M. Wilde, "Applications of position-based coding to classical communication over quantum channels," *J. Phys. A: Math. Theor.*, vol. 51, no. 44, p. 444002, Oct. 2018.

[20] M. Hayashi and N. Cai, "Universal classical-quantum multiple access channel coding," in *Proc. IEEE Int. Symp. Inf. Theory (ISIT)*, 2021, pp. 402–407.

[21] M. Hayashi and A. Vázquez-Castro, "Computation-aided classical-quantum multiple access to boost network communication speeds," *Phys. Rev. Applied*, vol. 16, p. 054021, Nov 2021.

[22] H. Shi and Q. Zhuang, "Computable limits of optical multiple-access communications," *Phys. Rev. A*, vol. 105, p. 022429, Feb 2022.

[23] H. Shi, M.-H. Hsieh, S. Guha, Z. Zhang, and Q. Zhuang, "Entanglement-assisted capacity regions and protocol designs for quantum multiple-access channels," *npj Quantum Information*, vol. 7, no. 1, pp. 1–9, 2021.

[24] R. Laurenza and S. Pirandola, "General bounds for sender-receiver capacities in multipoint quantum communications," *Physical Review A*, vol. 96, no. 3, p. 032318, 2017.

[25] A. Anshu, R. Jain, and N. A. Warsi, "On the near-optimality of one-shot classical communication over quantum channels," *Journal of Mathematical Physics*, vol. 60, no. 1, p. 012204, 2019.

[26] H. Aghaee and B. Akhbari, "Private classical information over a quantum multiple access channel: One-shot secrecy rate region," in *2020 10th Int. Symp. on Telecommunications (IST)*. IEEE, 2020, pp. 222–226.

[27] ——, "Classical-quantum multiple access wiretap channel," in *2019 16th Int. ISC (Iranian Society of Cryptology) Conference on Information Security and Cryptology (ISCISC)*. IEEE, 2019, pp. 99–103.

[28] A. K. Sinclair, E. Schroeder, D. Zhu, M. Colangelo, J. Glasby, P. D. Mauskopf, H. Mani, and K. K. Berggren, "Demonstration of microwave multiplexed readout of DC-biased superconducting nanowire detectors," *IEEE Trans. Appl. Supercond.*, vol. 29, no. 5, Aug. 2019.

[29] A. N. McCaughan, D. M. Oh, and S. W. Nam, "A stochastic SPICE model for superconducting nanowire single photon detectors and other nanowire devices," *IEEE Trans. Appl. Supercond.*, vol. 29, no. 5, Aug 2019.

[30] J. Lee, L. Shen, A. Cerè, T. Gerrits, A. E. Lita, S. W. Nam, and C. Kurtsiefer, "Multi-pulse fitting of transition edge sensor signals from a near-infrared continuous-wave source," *Rev. Sci. Instrum.*, vol. 89, no. 12, p. 123108, 2018.

[31] B. A. Bash, D. Goeckel, and D. Towsley, "Square root law for communication with low probability of detection on AWGN channels," in *Proc. IEEE Int. Symp. Inform. Theory (ISIT)*, Cambridge, MA, Jul. 2012.

[32] ——, "Limits of reliable communication with low probability of detection on AWGN channels," *IEEE J. Select. Areas Commun.*, vol. 31, no. 9, pp. 1921–1930, 2013.

[33] B. A. Bash, D. Goeckel, S. Guha, and D. Towsley, "Hiding information in noise: Fundamental limits of covert wireless communication," *IEEE Commun. Mag.*, vol. 53, no. 12, 2015.

[34] E. J. Anderson, S. Guha, and B. A. Bash, "Fundamental limits of bosonic broadcast channels," in *Proc. IEEE Int. Symp. Inform. Theory (ISIT)*, virtual, Jul. 2021.

[35] M. Reck, A. Zeilinger, H. J. Bernstein, and P. Bertani, "Experimental realization of any discrete unitary operator," *Phys. Rev. Lett.*, vol. 73, pp. 58–61, Jul. 1994.

[36] W. R. Clements, P. C. Humphreys, B. J. Metcalf, W. S. Kolthammer, and I. A. Walmsley, "Optimal design for universal multiport interferometers," *Optica*, vol. 3, no. 12, pp. 1460–1465, Dec 2016.

[37] E. J. D. Anderson and B. A. Bash, "Fundamental limits of thermal-noise lossy bosonic multiple access channel," 2022. [Online]. Available: https://arxiv.org/abs/2207.00139

[38] C. Weedbrook, S. Pirandola, R. García-Patrón, N. J. Cerf, T. C. Ralph, J. H. Shapiro, and S. Lloyd, "Gaussian quantum information," *Rev. Mod. Phys.*, vol. 84, pp. 621–669, May 2012.

[39] S. Guha, "Classical capacity of the free-space quantum-optical channel," Master's thesis, Massachusetts Institute of Technology, 2004.